Journal of The Electrochemical Society, **154** (3) B305-B309 (2007)
0013-4651/2007/154(3)/B305/5/$20.00 © The Electrochemical Society

Coplanar Electrodes Design for a Single-Chamber SOFC

Assessment of the Operating Parameters

X. Jacques-Bédard,[a] T. W. Napporn,[a,*,z] R. Roberge,[b] and M. Meunier[a]

[a]*Département de Génie Physique, École Polytechnique de Montréal, Montréal, Québec H3C 3A7, Canada*
[b]*Institut de Recherche d'Hydro-Québec, Varennes, Québec J3X 1S1, Canada*

Solid-oxide fuel cells (SOFC) made of conventional materials with coplanar interdigitated electrodes located on the same side of the electrolyte have been fabricated and tested in a uniform mixture of methane and air in order to evaluate the influence of various operating parameters on cell performances. Anode thickness of several hundred micrometers is required to reach good cell stability. Also, the relative positioning of the electrodes in regard to the gas flow should be optimized as the gas composition is modified after passage over the anode. This aspect is particularly important with stacked cells, due to the modification of the gas composition in the upstream portion of the stack. Enhanced performances of the single-side cell were obtained by decreasing the width of the electrodes and their spacing, which both have the effect of reducing the ohmic loss. Following this approach, performances of 40 mW cm^{-2} were recorded at 800°C using electrodes of 0.5 × 8 mm separated by a gap of 0.2 mm.
 [DOI: 10.1149/1.2424421]

Manuscript submitted July 14, 2006; revised manuscript received October 26, 2006. Available electronically January 10, 2007.

The idea of a single-chamber fuel cell was suggested several decades ago by Eyraud et al.[1] However, it was only in 1993 that Hibino demonstrated a cell capable of delivering significant currents.[2] Based on solid-oxide materials, it provided performance of 2.4 mW cm^{-2} at 950°C in a methane-air mixture. In the following years, most of the improvements were provided by: (*i*) changing the cell materials,[3-5] (*ii*) optimizing the operating conditions,[6-8] (*iii*) reducing the electrolyte thickness,[4,7,8] and (*iv*) operating with higher hydrocarbons.[4,9,10]

Nowadays, the single-chamber concept has gained interest among the fuel cell community and attracted new works on its practical implementation. Napporn et al.,[11] for example, have shown the importance of controlling the actual cell temperature and the gas flow around the electrodes. They also demonstrated that the conventional anode-supported cells developed for the planar solid-oxide fuel cell (SOFC) design are appropriate to single-chamber operation and provide outstanding performance up to 260 mW cm^{-2}.[12] However, during their operation the interaction between the methane-air mixture and the Ni-cermet anode already leads to exothermic combustion reactions, the most important being the partial oxidation one

$$CH_4 + \tfrac{1}{2}\,O_2 \rightarrow CO + 2H_2 \qquad [1]$$

Electrical as well as thermal efficiency must thus be considered for a complete analysis of such system. To date, however, few discussions have really tackled the subject through simple analysis of fuel utilization.[5,12-14] Under single-chamber conditions, this parameter is still very low with values below 10%. Nevertheless, some research groups are studying electrode materials to tailor their catalytic and electrocatalytic properties to the single-chamber conditions.[15,16] In general, these works are motivated by the simpler design single-chamber may have over the traditional dual-chamber configuration. Indeed, complex gas distribution through bipolar plates as well as sealing of the individual cells could be avoided with a resulting decrease in the cost of a fuel cell system. Also, the development of alternative cell design with both electrodes on the same side of the electrolyte is a challenge which can enhance the performance of such fuel cells. For instance, reduction of ohmic losses can be achieved by fabricating closely packed coplanar electrodes. When the electrode spacing is reduced, evidence of enhancement of the cell performance has already been proven by using rather simplified design.[17,18] More sophisticated designs with interdigitated electrodes have been proposed by various authors,[19,20] but require specific fabrication procedures[21] to reduce the electrode spacing significantly.

However, single-side cells that operate in single chamber are still at an early stage of development, and many questions remain before the elaboration of a fully practical design. While previous investigations have shown that anode thickness is a key factor that affects the performance and stability of single-chamber SOFC cells,[12] more detailed information is needed within the framework of developing suitable fabrication processes depending on the cell design. Optimal electrode geometry is another essential parameter. Indeed, if large electrode surface area serves to promote the fuel oxidation on the anode side,[5] its size would have to be adjusted to the increasing ohmic losses through the electrolyte.[18] Furthermore, while the gas composition is significantly modified through the catalytic oxidation of the fuel over the anode, the cell performance is expected to depend on the relative positioning of the electrodes in regard to the incoming gas flow. This concern also holds for stacked cells where the downstream portion of the stack is exposed to by-products resulting from fuel oxidation in the upstream portion of the stack. The purpose of this study is thus to clarify these points experimentally using simple, conventional SOFC materials.

Experimental

Fabrication.— Conventional materials are used for the main cell components, i.e., cathode, electrolyte, and anode. The $La_{0.8}Sr_{0.2}MnO_3$ cathode (LSM_{20}) powder was supplied by NexTech. The 0.2 mm thick 8YSZ electrolyte was provided by Marketech. The cathode slurry was prepared using the LSM_{20} powder mixed with terpineol as a solvent and polyvinyl butyral (PVB) as a bender. The cermet slurry, consisting of a Tosoh TZ-8Y powder ballmilled with fine NiO powder from Baker (nickelous oxide no. 2796-01), is prepared according to a state-of-the-art procedure. Slurries of both electrodes are tape casted onto the electrolyte followed by firing at 1200°C for 3 h. Two different NiO-based layers constitute the anode.

1. The first one, about 20 μm thick, contains 55 wt % nickel oxide/45 wt % YSZ, and is in contact with the electrolyte. According to Brown et al.[22] the electrochemical active region of the NiO-YSZ does not typically extend more than 10–20 μm from the anode-electrolyte interface.
2. The second one, richer in nickel (80% NiO and 20% YSZ w/w), with maximum thickness of 300 μm, is on the top of the first one. The purpose of this layer is to enhance the current collection.

As can be seen in Fig. 1, unit cells with different electrode dimensions and spacing were constructed. The electrode surface areas measured 8 × *w* mm^2 with *w* = 0.5, 1.0, 2.0, or 4.0 mm. The shortest gap *g* between the two electrodes ranged from *g* = 0.2 to 1.0 mm.

Stacked cells consisting of two to three sets of electrodes placed

* Electrochemical Society Active Member.
z E-mail: teko.napporn@polymtl.ca

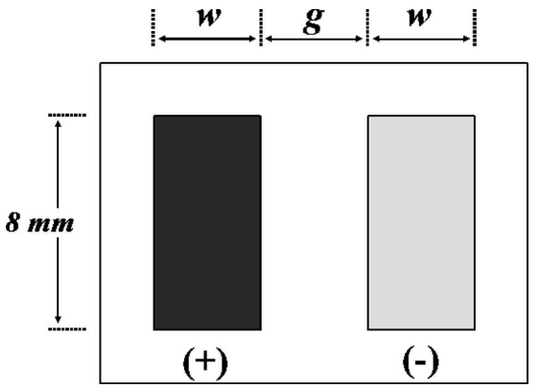

Figure 1. Schematic of the cells used in this study (top view). *w* and *g* are, respectively the width of the electrodes and the gap separating them.

on the same side of the electrolyte and connected in parallel by means of a gold paste were also fabricated. In that case, the electrodes measured 8 × 0.5 mm and were separated by a gap of 1 mm.

Setup.— The cells were tested under a setup described extensively in previous works.[11,12] Three different cell configurations based on the positioning of the electrodes relative to the incoming gas flow were tested. These positions are schematically drawn in Fig. 2 and are labeled position A, position C, and position AC according to which of the electrodes, anode (A), cathode (C), or both (AC) are first exposed to the gas flow. The same notation is also used for stacked cells. Before operating the cell, reduction of the cermet is carried out at a nominal temperature of 800°C, methane-to-oxygen ratio (R_{mix}) equal to 2.0 and a flow rate of 350 sccm. The inlet stream is made of methane and oxygen according to R_{mix} values and balanced with nitrogen to form the final methane + air mixture. Afterward, the cell is operated under various gas compositions keeping the furnace temperature constant at 800°C and the flow rate of 350 sccm. Polarization curves are established by drawing current in an ohmic load and monitoring the voltage through reference wires exiting from the cell. Due to the exothermic reactions involving methane and air in the reactor, cell temperature may depart from its nominal value upon introduction of the gas mixture. To closely follow the actual cell temperature, our setup includes a thermocouple that monitors the exhausted gas temperature, details of which can be found in Ref. 12.

Chemical analyses of the electrodes surface were carried out by time-of-flight secondary ions mass spectrometry (ToF-SIMS from Ion-ToF Company).

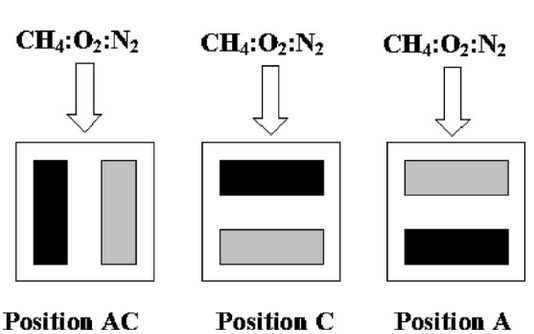

Figure 2. Different cell configurations determined by the electrodes positioning in regard to the gas flow.

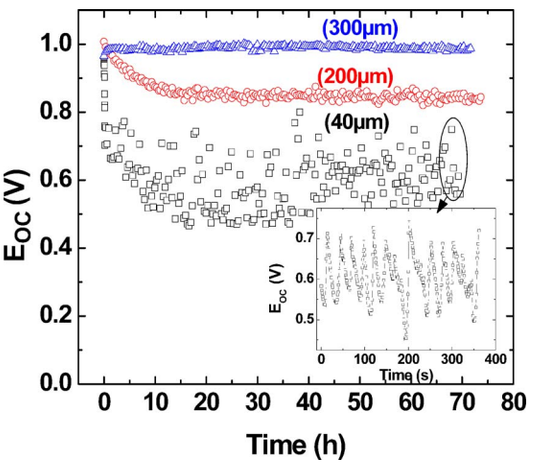

Figure 3. (Color online) Cell aging in OC voltage at R_{mix} = 2.0. Electrodes have width of w = 4.0 mm and are separated by a gap g = 1.0 mm. The anode is coated with a nickel-rich layer of various thicknesses.

Results and Discussion

A preliminary study was done to determine the best conditions for using our 80:20 NiO:YSZ overlayer. A number of experiments were thus performed recording the open-circuit (OC) voltage, E_{OC}. As shown in Fig. 3 for a unit cell with w = 4.0 mm and g = 1.0 mm in position C, the best stability was observed with a thick and highly electron conductive overlayer of 300 µm. However, the use of a thinner coating at the anode resulted in a strong decrease of E_{OC} right after the reduction of the cermet followed by oscillations, as shown in the inset of Fig. 3. During the partial oxidation of methane into syngas, Zang et al.[23] observed that oscillatory reactions accompanied temperature waves. The various oxidation states of the Ni and its interactions with the different compounds of the mixed gas could play a key role in the oscillatory processes. Furthermore, Tulenin et al.[24] have shown that some amount of oxygen and carbon are stored on the surface of Ni-containing catalysts and evolved during a cycle. Thus, for the cells having a thin anode, the oscillatory behavior of E_{OC} is probably due to the blocking of the electrochemical reactions sites by oxygen and carbon atoms or by the varying compositions of the gas mixture before it reaches the anode-electrolyte interface.

The loss of performance at E_{OC} may also depend on the chemical stability of the Ni-cermet anode toward the environment to which it is exposed. After 72 h testing in the reactive gas mixture, the anode appeared to have a visible white stripe about 0.5–1.0 mm wide near the fuel inlet. On the opposite, the fuel outlet region remained unaffected and presented a metallic aspect. These observations are in agreement with our previous work on anode supported cells.[25] As suggested by Gubner et al.,[26] this change has been attributed to the high reactivity of nickel in methane gas mixtures that contain high level of water vapor and which lead to the formation of volatile compounds. In the present investigation, similar changes also occurred on thicker anodes but to a lesser extent. ToF-SIMS chemical analyses, summarized in Table I, show the important decrease of the nickel content in the electrode close to the fuel inlet. Because of better cell stability, all of the following results have been obtained using a 300 µm thick overlayer at the anode.

The effect of electrode positioning relative to the incoming gas flow was studied in various methane-to-oxygen ratios for a unit cell with w = 4.0 mm and g = 1.0 mm. As shown in Fig. 4a, the cells with electrodes in position C and AC are characterized by a gradual decrease of E_{OC} with a lowering of R_{mix}. At R_{mix} = 0.5, a sudden drop below 100 mV occurs due to the cermet reoxidation (not shown on the graph). A similar trend was also reported for anode-

Table I. ToF-SIMS chemical analyses near the fuel inlet and fuel outlet following exposure of the cermet to an R_{mix} = 2.0 gas mixture for different time. Results are expressed as the ratio of the current generated by each ionic species.

	2 hours		72 hours	
	I_{Ni}/I_{Zr}	I_{NiO}/I_{ZrO}	I_{Ni}/I_{Zr}	I_{NiO}/I_{ZrO}
Near fuel inlet	8,33	2,42	0,56	0,37
Near fuel outlet	7,77	1,59	5,23	0,26

supported cells in a previous paper.[12] This typical behavior is however disrupted when the cell is placed in position A. Instead, in such a configuration, the data show that E_{OC} smoothly increases when R_{mix} is shifted from 2.0 to 0.88, while the usual drop is still observed below this limit. This noticeable departure is attributed to the sequence at which the electrodes are exposed to the gas flow. In position A, the reactive mixture is first exposed to the anode which burns up oxygen and fuel due to its catalytic activity for the partial oxidation of methane.[3,8,11] After its passage over the anode, the oxygen is partly consumed and thus diluted into the flowing mixture before it reaches the cathode. However, decreasing the methane-to-oxygen ratio helps in providing more oxygen to the cathode and in increasing the OC voltage. This particular situation does not occur for positions C or AC because the cathode material (LSM) has no activity for the partial oxidation of methane.[3,8,11] As expected, the electrode positioning affects in a similar manner the maximum power densities measured for the various gas compositions (Fig. 4b). The best results are obtained in position C and AC in methane-rich mixture, while a significant drop is observed in position A. Our temperature monitoring confirmed that such a discrepancy is not the result of dissimilar cell temperatures. The lower performance obtained in position A is thus explained by the promotion of the oxygen consumption before the gas mixture reaches the cathode, as discussed above.

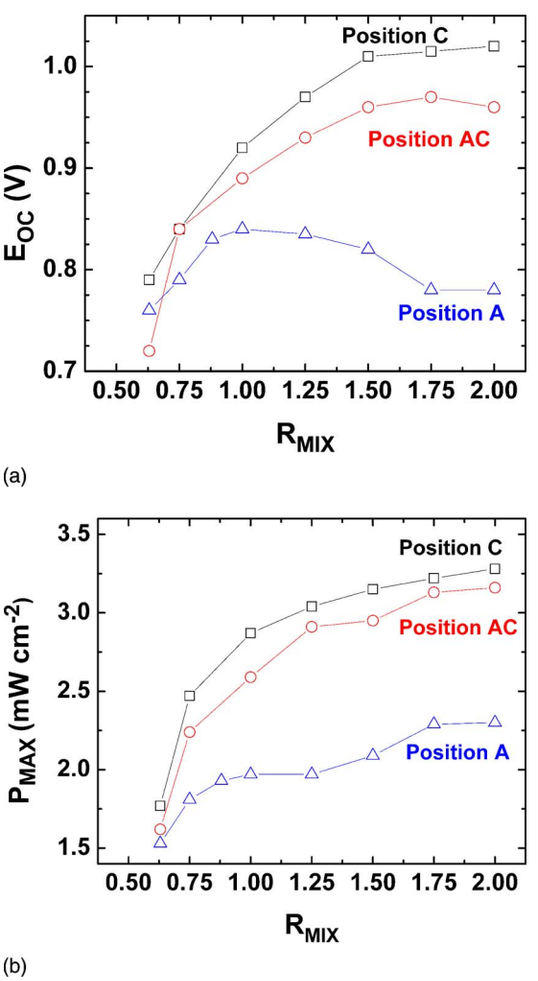

Figure 4. (Color online) (a) OC voltage and (b) maximum specific power of the unit cell with w = 4.0 mm and g = 1.0 mm operated in various gas compositions and cell configurations.

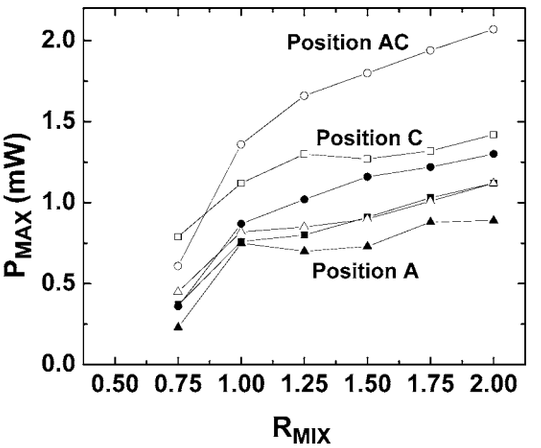

Figure 5. Maximum specific power delivered by stacked cell constituted of two (filled symbols) or three (open symbols) sets of electrodes for various gas compositions and cell configurations with w = 0.5 mm and g = 1.0 mm.

The conclusions drawn from the results of the unit cell may also apply to stacked cells formed with two or three sets of coplanar electrodes on the electrolyte. For example, Fig. 5 presents the maximum power densities delivered by stacked cells in various positions and gas compositions. In this case, position AC alone leads to the most acceptable results. In position A and C, the gas content is indeed affected by its passage over the prior set of electrodes, and the performance is decreased.

The advantage of using stacked cells compared to unit cell was also studied. Figure 6 shows the E,P vs I curves. In the case of the voltage-current curves, a limitation in the activation region is occur-

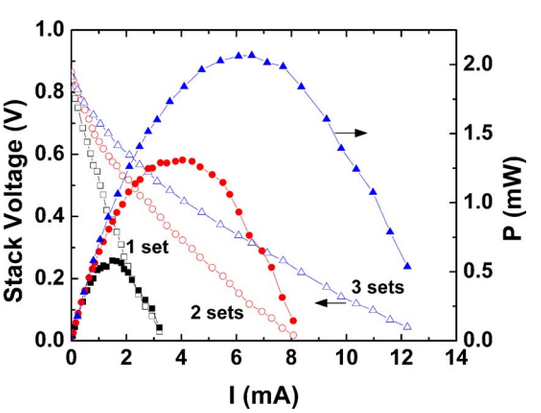

Figure 6. (Color online) Discharge properties at R_{mix} = 2.0 of stacked cells constituted of one to three sets of electrodes in position AC with w = 0.5 mm and g = 1.0 mm.

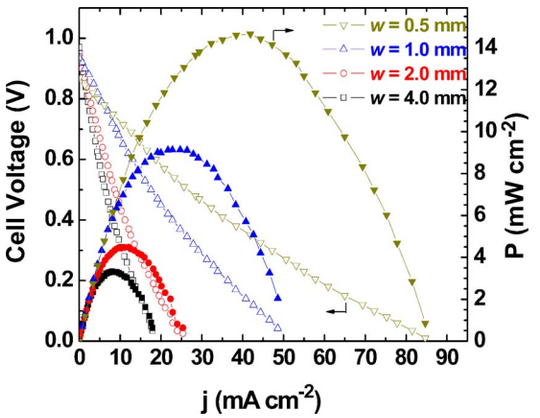

Figure 7. (Color online) *E-j* characteristics at R_{mix} = 2.0 for the unit cell in position C for various electrode widths *w* separated by a gap *g* = 1.0 mm.

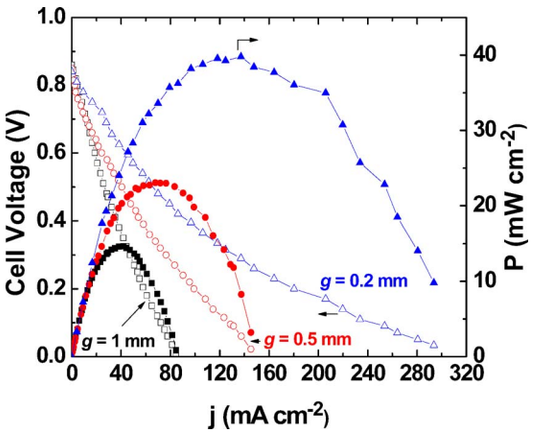

Figure 8. (Color online) *E-j* characteristics at R_{mix} = 2.0 for the unit cell in position C with *w* = 0.5 mm for various gap distances *g* between the electrodes.

ring. This behavior might be due to the absence of a functional layer (LSM-YSZ) at the interface with the electrolyte. Here, only a pure LSM_{20} cathode layer was used. Nonetheless, the discharge properties of two sets of coplanar electrodes show that the maximum power is more than twice that of the unit cell. In this case, the number of electrochemically active sites in an electrode located in the middle of the stack is increased because it is surrounded on each side by electrodes of the opposite type. This occurs because it is expected that the whole surface of the electrode does not contribute equally to the electrochemical reactions. In the case of the unit cell, the most active region should be located where the electrodes are closest to each other, which minimizes the ohmic resistance associated with the ion path. This effect can be seen in Fig. 7, which represents the discharge properties of the unit cell in position C for various electrode width *w* keeping *g* equal to 1.0 mm. Cells with larger electrode area show reduced performances in comparison to those with smaller *w* values. For the cell width *w* = 4.0 mm, the longest distance between the electrodes is $2w + g = 9.0$ mm, but only 2.0 mm for the cell with *w* = 0.5 mm. These results indicate that the electrochemical activity of the electrodes is not distributed equally over its surface but depends on the TPB site in the active layer. This point has been discussed by Fleigh et al.,[27] who have demonstrated on a theoretical basis that the performances of the single-side cell are strongly affected by the electrode size. This parameter influences the ohmic resistance associated with the path of the ion under the electrode surface before it reaches the reaction site.[27] Their calculations suggest that electrode width and spacing must be designed taking into account the electrode reaction resistance to reach optimal performance for this type of cell.[27]

The size of the electrodes also influences the overall cell behavior in different manners. The results of Fig. 7 show, for example, that E_{OC} is higher for cells having larger electrode areas. This is due to better conversion of the methane gas over the anode.[5] Moreover, Table II indicates that the aging process is more effective going to smaller electrode width. This is seen either from the E_{OC} drop observed on the cell width *w* = 0.5 mm after 72 h testing at OC voltage, or from the discharge properties measured before and after the aging test where the maximum delivered power densities measured were 82, 67, 49, and 48% of their original values for the cells with *w* = 4.0, 2.0, 1.0, and 0.5 mm, respectively. Because the size of the affected area that contains the white stripe as discussed previously was measuring around 0.5 mm in width in every case, the electrode area remaining unaffected following the aging test was more important for cells with larger electrode size. For the cell width *w* = 0.5 mm, the whole surface of the anode appeared white after the test while most of the electrodes surface remained unaffected for the cell width *w* = 4.0 mm.

In addition to a reduction of the electrode width alone, improved performance of single-side cell may be achieved by reducing the spacing between the electrodes. Figure 8 illustrates the discharge properties of the unit cell where *w* = 0.5 mm and *g* is varied from 1.0 mm down to 0.2 mm. The largest power density of 40 mW cm^{-2} was obtained with *g* = 0.2 mm. This corresponds to the cell having the smallest ohmic resistance. The reduction of *g* by a factor of 5 resulted in an increase of performance by a factor of 2.7. This compares favorably to the values reported by Hibino et al.,[7] who found an increase of the maximum power density of their single-side cell from 65 to 143 mW cm^{-2} by reducing the gap between their electrodes from 3.0 to 0.5 mm. Also, the performance of 40 mW cm^{-2} with *g* = 0.2 mm is lower than that of 89 mW cm^{-2} reported earlier[11] in the same conditions using double-sided cell with an electrolyte 0.2 mm thick. The effective ohmic resistance for the single-side cell must, however, take into account the size of the electrode (*w* = 0.5 mm). Additional increase of the single-side cell performance could be achieved by reducing further the gap separating the electrodes. The deposition of electrodes with *g* below 0.2 mm would then require the development of special preparation procedures.

Table II. Variation of the OC voltage and maximum specific power of the unit cell with *g* = 1.0 mm and various width *w* before and after aging for 72 h at R_{mix} = 2.0.

	w = 4.0 mm		*w* = 2.0 mm		*w* = 1.0 mm		*w* = 0.5 mm	
	Before	After	Before	After	Before	After	Before	After
E_0 (volts)	0.97	0.99	0.94	0.93	0.93	0.93	0.87	0.82
P_{Max} (mW cm^{-2})	3.3	2.7	4.5	3.0	9.1	4.5	14.7	7.0

Conclusion

Various parameters of the single-sided cell operated in a single chamber were investigated in a methane-air mixture at 800°C. The thickness of the anode could be adjusted to reach good cell stability for short periods of test. However, questions arose concerning the use of a NiO-YSZ cermet for practical cells because the material deteriorated rapidly in methane-oxygen mixtures at elevated temperature. Due to the catalytic activity of the anode for the fuel oxidation, the relative positioning of the electrodes toward the gas flow should be optimized both for the unit cell and the stacked cells. Also, it has been demonstrated that reducing the electrode area and the electrode spacing is appropriate for enhancing cell performance. However, electrode width cannot be indefinitely reduced because aging of the anode becomes more effective in this case, at least for the material used in this study.

Several issues arose from this work concerning the practicality of the single-sided design. Suitable deposition techniques for making thick anodes closely spaced to the cathodes need to be developed. The performances of larger cell should be evaluated to fully account for the feasibility of the single-sided cell. Finally, aging of the NiO-YSZ cermet in a methane-air mixture at elevated temperatures raises fundamental problems. The long-term development of the single-chamber SOFC should aim at the elaboration of new electrode materials more suitable to the special operating conditions of single-chamber SOFCs.

Acknowledgments

The authors thank Jean-Paul Levesque for his technical help. The Natural Sciences and Engineering Research Council of Canada and the Hydro-Québec Research Institute are acknowledged for their financial support.

References

1. C. Eyraud, J. Lenoir, and M. Géry, *Acad. Sci., Paris, C. R.*, **252**, 1599 (1961).
2. T. Hibino and H. Iwahara, *Chem. Lett.*, **7**, 1131 (1993).
3. T. Hibino, S. Wang, S. Kakimoto, and M. Sano, *Electrochem. Solid-State Lett.*, **2**, 317 (1999).
4. T. Hibino, A. Hashimoto, T. Inoue, J.-I. Tokuno, S.-I. Yoshida, and M. Sano, *Science*, **288**, 2031 (2000).
5. T. Hibino, A. Hashimoto, M. Yano, M. Suzuki, S.-I. Yoshida, and M. Sano, *J. Electrochem. Soc.*, **149**, A133 (2002).
6. T. Hibino, Y. Kuwahara, and S. Wang, *J. Electrochem. Soc.*, **146**, 2821 (1999).
7. T. Hibino, H. Tsunekawa, S. Tanimoto, and M. Sano, *J. Electrochem. Soc.*, **147**, 1338 (2000).
8. T. Hibino, S. Wang, S. Kakimoto, and M. Sano, *Solid State Ionics*, **127**, 89 (2000).
9. T. Hibino, A. Hashimoto, T. Inoue, J.-I. Tokuno, S.-I. Yoshida, and M. Sano, *J. Electrochem. Soc.*, **147**, 2888 (2000).
10. T. Hibino, A. Hashimoto, T. Inoue, J.-I. Tokuno, S.-I. Yoshida, and M. Sano, *J. Electrochem. Soc.*, **148**, A544 (2001).
11. T. W. Napporn, F. Morin, and M. Meunier, *Electrochem. Solid-State Lett.*, **7**, A60 (2004).
12. T. W. Napporn, X. Jacques-Bédard, F. Morin, and M. Meunier, *J. Electrochem. Soc.*, **151**, A2088 (2004).
13. I. C. Stefan, C. P. Jacobson, S. J. Visco, and L. C. De Jonghe, *Electrochem. Solid-State Lett.*, **7**, A198 (2004).
14. T. Suzuki, P. Jasinski, V. Petrovsky, H. U. Anderson, and F. Dogan, *J. Electrochem. Soc.*, **152**, A527 (2005).
15. Z. Shao and S. M. Haile, *Nature (London)*, **431**, 170 (2004).
16. A. Tomita, D. Hirabayashi, T. Hibino, M. Nagao, and M. Sano, *Electrochem. Solid-State Lett.*, **8**, A63 (2005).
17. T. Hibino, K. Ushiki, T. Sato, and Y. Kuwahara, *Solid State Ionics*, **81**, 1 (1995).
18. T. Hibino, A. Hashimoto, M. Suzuki, M. Yano, S.-I. Yoshida, and M. Sano, *J. Electrochem. Soc.*, **149**, A195 (2002).
19. W. van Gool, *Philips Res. Rep.*, **20**, 81 (1965).
20. T. Hibino, K. Ushiki, and Y. Kuwahara, *Solid State Ionics*, **91**, 69 (1996).
21. S.-J. Ahn, J. Moon, J.-H. Lee, and J. Kim, in *Proceedings of Fuel Cells Science & Technology 2004, Scientific Advances in Fuel Cell Systems*, Munich, Oct 6–7, 2004.
22. M. Brown, S. Primdhal, and M. Mogensen, *J. Electrochem. Soc.*, **147**, 475 (2000).
23. X. Zhang, D. O. Hayward, and D. M. P. Mingos, *Catal. Lett.*, **86**, 235 (2003).
24. Y. P. Tulenin, M. Y. Sinev, V. V. Savkiv, and V. N. Korchak, *Catal. Today* **91–92**, 155 (2004).
25. X. Jacques-Bédard, T. W. Napporn, R. Roberge, and M. Meunier, *J. Power Sources*, **153**, 108 (2006).
26. A. Gubner, H. Landes, J. Metzger, H. Seeg, and R. Stübner, in *Solid Oxide Fuel Cells V*, U. Stemming, S. C. Singhal, H. Tagawa. and W. Lehnert, Editors, PV 97-40, p. 844, The Electrochemical Society Proceedings Series, Pennington, NJ (1997).
27. J. Fleigh, H. L. Tuller, and J. Maier, *Solid State Ionics*, **174**, 261 (2004).